The role of insert devices on enhancing heat transfer in a flat-plate solar water collector

A. García (*), R. Herrero-Martin, J.P. Solano, J. Pérez-García

Departamento de Ingeniería Térmica y de Fluidos, Universidad Politécnica de Cartagena, Cartagena (Spain)

alberto.garcia@upct.es; ruth.herrero@upct.es; juanp.solano@upct.es; pepe.perez@upct.es;

Abstract

This work presents a comparative experimental study of heat transfer enhancement in a flat-plate solar water collector using insert devices. Three wire-coils and three twisted-tapes were selected with representative geometrical characteristics typically employed in industrial applications. Isothermal pressure drop tests were carried out to obtain the fully-developed Fanning friction factor for a range of Reynolds numbers Re = [80-9000]. The increase in friction factor in comparison to smooth tube was computed for all the devices. Depending on Reynolds number and insert geometry f_i/f_s values ranged from 1.3 to 79.8. Furthermore, detailed temperature profiles were obtained for different sections along the absorber plate and the risers for five different mass flow rates covering the Reynolds range from [400-2500]. The increase of the inner heat transfer coefficient by the inserts caused an important decrease of the absorber temperature. At increasing mass flow rates (from Re≈1000), all the inserts showed a very similar thermal performance which make them suitable for inserting within harp-type solar collectors, where pressure drop is not a constraint. The best inserts TT03, WC01 and WC02 gave at Re≈1500 maximum absorber temperature decreases (insert vs smooth tube) of 5.05˚C, 5.40˚C and 5.34˚C. In serpentine-type solar collectors, due to pressure drop constraints, the wire coil WC01 with a moderate pitch to wire-diameter ratio (p/d=1.5 and e/d=0.07), is the best specimen to insert. WC01 presents a moderate pressure drop increase (f_i/f_s =2.8 at Re≈1000), an early promotion of turbulent flow (at Re≈700), and a significant reduction of the absorber temperature (decreasing 4.84˚C vs smooth tube at Re≈1000).

Keywords: Flat-plate solar collector; Heat transfer enhancement; Wire-coil inserts; Twisted tape inserts;

1. Introduction

A thermal solar collector is a special kind of heat exchanger that transforms solar radiant energy into heat. Flat-plate collectors can be designed for applications requiring energy delivery at moderate temperatures. The major applications of these units are in solar water heating, building heating, air conditioning and heat transfer equipment for industrial processes [1]. Enhancement of the performance of solar collectors can be achieved by using different methods and techniques [2] such as employing innovative designs [3-7] and/or increasing the thermal conductivity of the working fluid [8-12].

Regarding liquid solar collectors, the use of passive heat transfer enhancement techniques [13] is gaining attention. Recently, Balaji et al [14-15] employed passive techniques (rod and tube velocity enhancers) in flat plate solar collectors and reported a rise in efficiency with minimum increase in pumping power consumptions. Commonly, the flow inside the risers is laminar for the typical operating conditions [1] and devices such as twisted-tape [13] and wire-coil inserts [16] have proved their suitability for increasing the inner tube convective heat transfer coefficient.

Twisted tapes inserts promote high heat transfer rates by the generation of a helical swirl increasing fluid mixing. Their effective use has been widely reported [17-18]. Twisted tapes are the most employed passive technique to augment the heat transfer in solar water heating systems. The heat transfer in the solar collector with twisted tape is found to be better than the conventional plain tube collector [13]. Kumar and Prasad [19] computed the thermal performance of a serpentine collector inserting different twisted-tapes. Later, Jaisankar et al [20] also performed an experimental investigation of heat transfer, friction factor and thermal performance on a harp type solar panel with twisted-tape insert devices. More recently, Pavendan et al [21] fitted seven types of cross twisted-type inserts into a solar panel. All the previous mentioned works were carried out in turbulent flow using water as the working fluid and reported a reduction of heat losses and an increase in thermal performance in all the studied cases. In a recent work, Sundar et al [22] combined the use of twisted tape inserts and nanofluids in a solar water heater. They reported thermal performance increases that largely outweighed pressure drop losses.

Regarding laminar flow studies, Jaisankar et al [23-28], carried out several studies on thermosyphon solar water heaters, introducing helical, left-right, twist with rod and spacer twist inserts. They reported [28] that the heat transfer in the modified collector was higher than in the standard collector and this was maximized when using minimum twist ratio specimens. Saravanan et al [29-30] also inserted twisted tapes in a V-trough solar water heater. The authors stated that the use of square and V-cut twisted tapes provides additional disturbances in the fluid flow that enhances the thermal performance.

Some recent reviews dealing with the thermal performance improvement in solar water heating systems do not even mention wire coils as elements to consider within this field of work [13]. However, Sheikholeslami et al [31] mentioned that wire coil gives better overall performance than other inserts, if the pressure drop penalty is considered. Wire-coil inserts have proved their effectiveness in laminar and low turbulent flow [32]. However in turbulent flow, wire-coil inserts are not as efficient as corrugated and dimpled tubes [33-34]. In laminar flow, wires coils accelerate considerably the transition to turbulence flow [35-36]. This fact makes these devices specially suitable for being inserted in solar collectors. In [37], the present authors studied heat transfer enhancement in a tube-on-sheet solar panel with wire-coil inserts using TRNSYS. The enhanced collector increased the thermal efficiency values by 4.5%. In a later work, García et al [38] established experimentally the enhancement potential of wire-coils inserted within the riser of a solar water collector. The modified collector standardized thermal efficiency was increased by 14-31%, depending on the mass flow rate, in comparison with a standard collector. More recently, Huertas et al [39] developed an experimental study on liquid solar collectors with two wire-coil inserts to analyse the Fanning friction factor and Nusselt number using a mixture of propylene-glycol/ water as working fluid. The authors concluded that using wire-coil inserts was a suitable enhancement technique in flat-plate solar collectors.

Regarding comparative studies, Hobbi and Siddiqui [40] conducted an indoor experimental study to investigate the impact of inserting several devices (twisted tapes, wire coils and conical ridges) on the thermal performance of a flat-plate solar collector. In contradiction with all the previous studies mentioned.they did not observe any significant heat transfer enhancement They reported that the inserts mitigated the strong buoyancy forces naturally present in the standard collector. However, in a later work [41], the same authors carried out an experimental study at lower Rayleigh numbers (closer to the real operating conditions in solar collectors). They employed different insert devices (twisted-tapes, wire coils attached and not-attached to the tube wall, concentric and conical coils and mesh inserts) and observed that all the inserts enhanced the Nusselt number. Regarding the influence of collector inclination on the performance, no significant impact on the Nusselt number enhancement was observed.

According to the literature review undertaken, there is a scarcity of experimental studies comparing the thermal performance of different passive techniques in solar collectors. This article presents an experimental study of three twisted tapes and three wire coils specimens that were inserted within a solar collector tube. Friction factor results and the axial and longitudinal temperature evolution within the riser and absorber are analysed in order to address the viability of using inserts to enhance heat transfer in solar collectors. A predictable link between the friction factor and the flow patterns is reported, and the impact on heat transfer results is addressed. Valid criteria to select the most adequate insert device in actual flat plate solar collectors are provided according to their operating conditions.

Nomenclature

c_p	[J/kg K]	Specific heat
d	[m]	Inside tube diameter
e	[m]	Wire coil diameter/ twisted tape thickness
f	[-]	Fanning friction factor
Gr	[-]	Grashof number $Gr=g\beta d^4 q''/(\mu/\rho)^2 k$
k	[W/mK]	Thermal conductivity
L	[m]	Tube length, heat transfer experiments
l_p	[m]	Tube length, pressure drop experiments
$\dot{m}$	[kg/s]	Mass flow rate
p	[m]	insert pitch
ΔP	[Pa]	Pressure drop
Pr	[-]	Prandtl number
q''	[W/m^2]	Heat flux
Re	[-]	Reynolds number
Re_{sw}	[-]	Reynolds Swirl number $Re_{Sw}= Re\cdot(\pi/(\pi-4(e/d)))\cdot(1+(\pi/2y)^2)^{1/2}$
Ri	[-]	Richardson number $Ri=Gr/Re^2$

Sw	[-]	Swirl number $Sw=(Re/y^{0,5})\cdot(\pi/(\pi-4(e/d)))\cdot(1+(\pi/2y)^2)^{1/2}$
T	[K]	Temperature
y	[-]	Twist ratio y=p/d
Special characters		
β	[K^{-1}]	Thermal expansion coefficient
ρ	[kg/m^3]	Fluid density
μ	[Pa s]	Fluid dynamic viscosity
Subscripts		
a		Absorber plate
i		Insert
in		Tube inlet
out		Tube outlet
s		Smooth
w		Tube wall
f		Fluid

2. Experimental setup

2.1 Specimens tested

Fig. 1 shows the helical wire coil and the twisted tape inserted in a smooth tube, respectively. In the figure *p* represents a 360º turn in wire coils and the 180º helical twist pitch in twisted tapes.

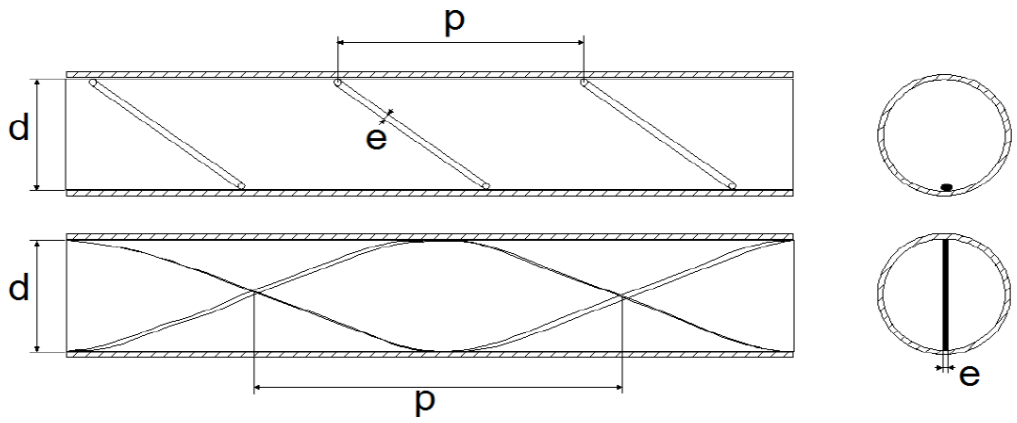

Figure 1 Sketch of the inserts: a wire coil inserted in a smooth tube (upper) and a twisted tape inserted in a smooth tube.

The geometrical parameters can be arranged in dimensionless form as pitch and wire-diameter, *p/d* and *e/d*. Three different geometries have been selected for the present study, as shown in Table 1. These inserts are representative of those typically employed in real applications.

Table 1 Geometrical parameters of the specimens

Type	d (mm)	p (mm)	e (mm)	p/d	e/d	p/e
Wire-coil						
WC01	7	10.5	0.5	1.5	0.07	21.0
WC02	7	7.5	1.4	1.1	0.20	5.3
WC03	7	7.0	2.0	1.0	0.28	3.5
Twisted-tape				y		
TT01	7	126.0	0.7	24.0	0.10	180.0
TT02	7	84.0	0.7	12.0	0.10	120.0
TT03	7	42.0	0.7	6.0	0.10	60.0

2.2 Pressure drop loop

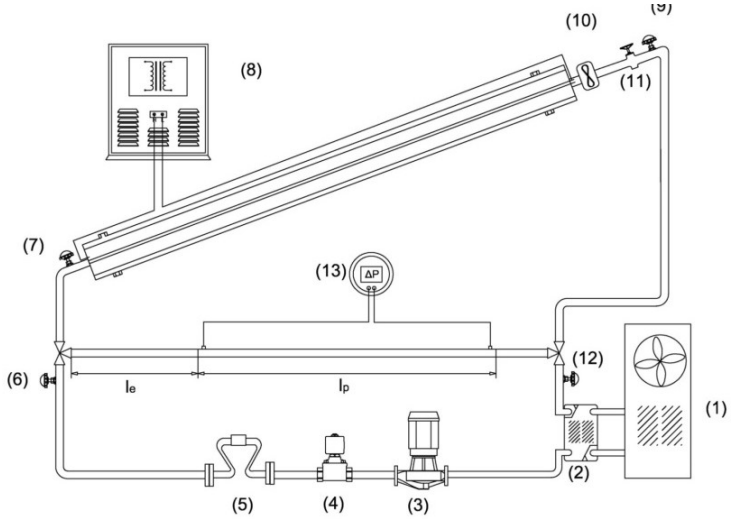

Figure 2 Schematic diagram of the experimental set up.

Key for figure 2

(1) Cooling machine (2) plate heat exchanger (3) circulating pump (4) electro-valve (5) Coriolis flow-meter (6), (7), (9) and (12) RTD sensors (8) autotransformer (10) turbine flow-meters (11) precision fine-tune valve (13) differential pressure sensor.

Fig. 2 shows the main components of the test rig employed in the present work. A detailed description of the experimental facility can be found in reference [20]. Pressure drop measurements were carried out in the lower loop under isothermal conditions. This horizontal test section contained a copper tube of 1.4m length which was fully insulated and 7 mm inner diameter fitted with the insert devices. The inserts were attached to the tube wall in order to assure no geometrical or positional variation. The measurement sections consisted of four pressure taps separated by 90º and were connected to a SMAR® differential pressure sensor. Two differential pressure transducers of different full scales were used to assure the accuracy of the experiments. The test section length was l_p = 200 diameters and was preceded by a hydrodynamically developing region of l_e = 60d length. Submerged RTDs were employed to measure the inlet and outlet fluid temperatures T_{in} and T_{out}. All the experimental data was collected through an Agilent® data acquisition model 34980A.

The experimental set-up allowed the Fanning friction factor to be obtained for a continuous range of Reynolds number between 80 and 9000.

The Fanning friction factor *f* was determined from the fluid mass flow rate and pressure drop measurements by means of the equation

$$f = \frac{\Delta P \cdot d^5 \cdot \pi^2 \cdot \rho}{32 \cdot l_p \cdot \dot{m}^2} \quad (1)$$

2.3 Heat transfer loop

Heat transfer tests were carried out in the upper loop of the facility (solar collector loop). The collector was fully insulated, as shown in Fig. 3.

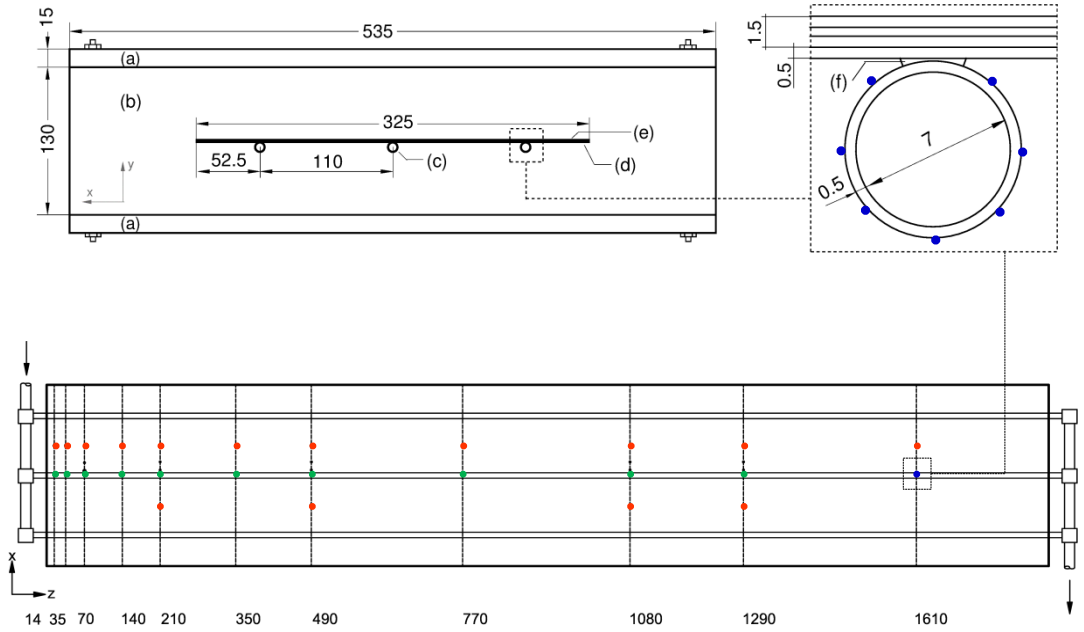

Figure 3 Upper left: cross-section of the solar collector rig for tube-side heat transfer measurements.

Key for figure 3

(a) Wood frame; (b) Insulation; (c) copper tubes; (d) absorber; (e) heater; (f) welding. *Bottom:* top-view of the plate absorber. Positions of the thermocouples are indicated with bullets. *Upper right*: Detail of the placing of tube wall thermocouples at axial position 1610 mm (“section J”). All dimensions in mm.

The experimental rig was designed to reproduce the conditions found in typical operating solar collectors . A uniform heat flux of 800 W/m^2 was applied to the absorber plate (1.8 m × 0.325 m) by tailored-made resistance heaters ,provided by Watlow® silicon-rubber The total power dissipated in the resistance heaters was regulated by an adjustable auto-transformer by Torivac® The copper riser of 7 mm inner diameter was electrowelded to the absorber plate.

Fig. 3 (bottom) represents the lay-out with the location of the thin film type-T thermocouples glued on the rear side of the absorber plate. In order to obtain the cross sectional temperature variation in the absorber plate four sections at different axial positions were instrumented (210, 490, 1080 and 1290 mm) together with the temperature in the bottom of the tube. Three sensors were located in the absorber panel

at -55 mm, -25 mm and -10 mm distances measured from the central riser. Another wall probe was located at the lowest point of the riser tube (lowest circumferential location 180º). Six additional axial sections measured the temperature in the centre of the absorber plate between two consecutive tubes (Section A). At an axial position of 1610 mm (Section J), seven thermocouples were peripherally spaced at the outside wall of the centre tube (see detail in Fig. 3 upper-right

2.3.1 Operating conditions

The experimental rig was designed to model the standard working conditions for flat plate solar collectors working in the south of Spain. Typically collectors use a mixture of propylene-glycol and water of 25% in volume as the heat transfer fluid. The fluid operates within temperature range of 15 °C-70 °C,with Re=300-1100 and Ri=0.1-0.2' This results in forced convection laminar flow heat transfer in the collector tubes. For a typical mass flow rate per tube of 16 kg/h, a solar collector working to supply water at 60ºC to the storage tank would be working at Pr 7.2 and Re around 900 with Ri<0.2.

In the present study, the operating conditions of solar collectors were reproduced using water as the working fluid. The use of water avoids the disadvantages of employing glycol mixtures, such as: the uncertainty on computing thermophysical properties, installation aging or the additive requirements to avoid corrosion, among others. To minimize heat losses, the inlet mean fluid temperature was regulated to a value very close to the ambient temperature (T_{in} = 15 ºC). Five different values of mass flow rate per tube are studied: 9 kg/h, 13 kg/h, 21 kg/h, 32 kg/h and 50 kg/ h.

The fluid flow parameters in the present study at the inlet and the outlet of the risers are summarized in Table 2:

Table 2 Dimensionless parameters at the inlet and outlet of the risers for the studied mass flow rates

	Re	Pr	Gr	Ri
$\dot{m}_1 = 9$ kg/h	400-570	8.1-5.4	18160-73050	0.11-0.22
$\dot{m}_2 = 13$ kg/h	570-740	8.1-6.1	18160-50340	0.05-0.09
$\dot{m}_3 = 21$kg/h	930-1050	8.1-7.0	18160-32230	0.02-0.03
$\dot{m}_4 = 32$ kg/h	1400-1600	8.1-7.0	18160-32230	≈0.01
$\dot{m}_5 = 50$ kg/h	2200-2500	8.1-7.0	18160-32230	≈0.01

In this study, according to the Richardson number calculation the prominent heat transfer mechanism within the risers is forced convection. A 21 kg/h water mass flow rate gives the closest match to the typical operational conditions of a 25% glycol mixture The maximum mass flow of 50 kg/h illustrates the affect of a change in flow regime in smooth tubes to help to correctly understand the results.

3. Results and discussion

3.1 Friction Factor results

Prior to studying the effects of inserts, the smooth tube pressure drop tests were carried out in order to verify measurement accuracy. The results shown an excellent agreement between the experimental results and the analytical solution for laminar flow and the Blasius equation for turbulent flow. It is remarkable that the presence of a perfectly defined transition region between both regimes is illustrated. The results are shown in Fig. 4 and also in Fig. 5.

3.1.1 Twisted-tape friction factor results

In Fig. 4 a comparison between the experimental results for the three twisted-tape inserts studied and the smooth tube isothermal friction factor are shown throughout the Reynolds number range studied.

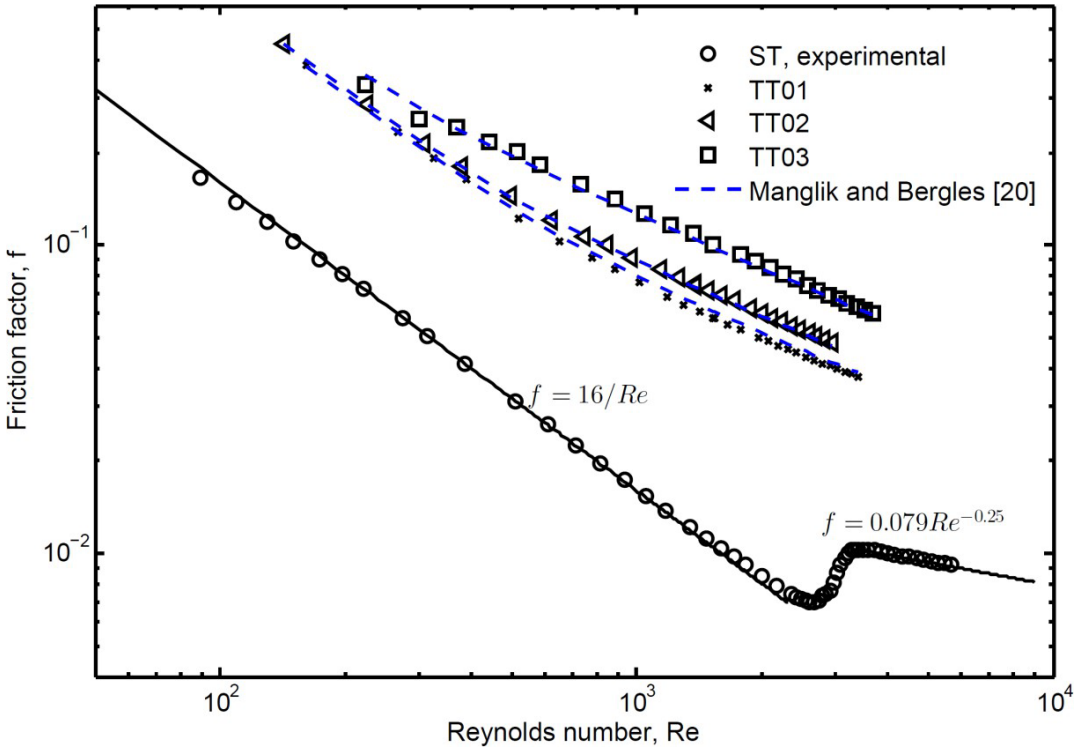

Figure 4: Comparison of twisted-tapes and smooth tube isothermal friction factor

The twisted tapes show a characteristic continuous trend, without abrupt changes in the slope of the friction factor curve. These inserts create laminar flow as they induce a secondary fluid motion restraining turbulence development. This fact can be observed in the lack of the characteristic discontinuity that represents the onset of turbulence in the smooth tube. The present results agree very well with the correlation proposed by Manglik and Bergles [42] which covers laminar, transition and turbulent flow in a single equation:

$$f_l = \frac{15.767}{Re}\cdot\left(1 + 10^{-6}\,Sw^{2.55}\right)^{1/6}\cdot\left(1 + (\pi/2y)^2\right)\cdot\left(\frac{\pi + 2 - 2\delta/d}{\pi - 4\delta/d}\right)^2\cdot\left(\frac{\pi}{\pi - 4\delta/d}\right)$$

$$f_t = \frac{0.0791}{Re^{0.25}}\cdot\left(\frac{\pi}{\pi - 4\delta/d}\right)^{1.75}\cdot\left(\frac{\pi + 2 - 2\delta/d}{\pi - 4\delta/d}\right)^{1.25}\cdot\left(1 + \frac{2.752}{y^{1.29}}\right)$$

$$f = \left(f_l^{10} + f_t^{10}\right)^{0.1} \qquad (2)$$

As would be expected, for the same Reynolds number values ,the friction factor increases as the twist ratio decreases. The twisted tapes TT01 and TT02 show a similar behaviour and different to TT03 in terms of heat transfer.

The laminar flow in twisted tape inserts can be characterised by the Swirl parameter. However, under a turbulent flow regime (typically Sw over 1400-2000) this parameter is not representative due to the inherent enhanced mixing by turbulence eddies. This makes the scaling of tape-induced swirl not applicable (as reported by Manglik and

Bergles, [43]). Table 3 shows the corresponding Sw parameters at the flow regimes studied in the present research.

Table 3 Sw values for the flow regimes evaluated

	TT01		TT02		TT03	
	Re_{Sw}	Sw	Re_{Sw}	Sw	Re_{Sw}	Sw
$\dot{m}_1 = 9$ kg/h	480	98	550	161	560	229
$\dot{m}_2 = 13$ kg/h	700	143	710	207	790	324
$\dot{m}_3 = 21$kg/h	1050	214	1050	304	1150	473
$\dot{m}_4 = 32$ kg/h	1550	316	1570	453	1700	705
$\dot{m}_5 = 50$ kg/h	2360	482	2410	697	2600	1067

For the mass flow rates under study the Sw numbers computed indicate the presence of a laminar flow regime. More specifically, the Sw ranges between the swirl transition regime (70-250) up to fully developed swirl flow regime (250-1400).

3.1.2 Wire-coil friction factor results

The experimental friction factor results for the three wire coil inserts and the smooth tube are depicted in Fig. 5.

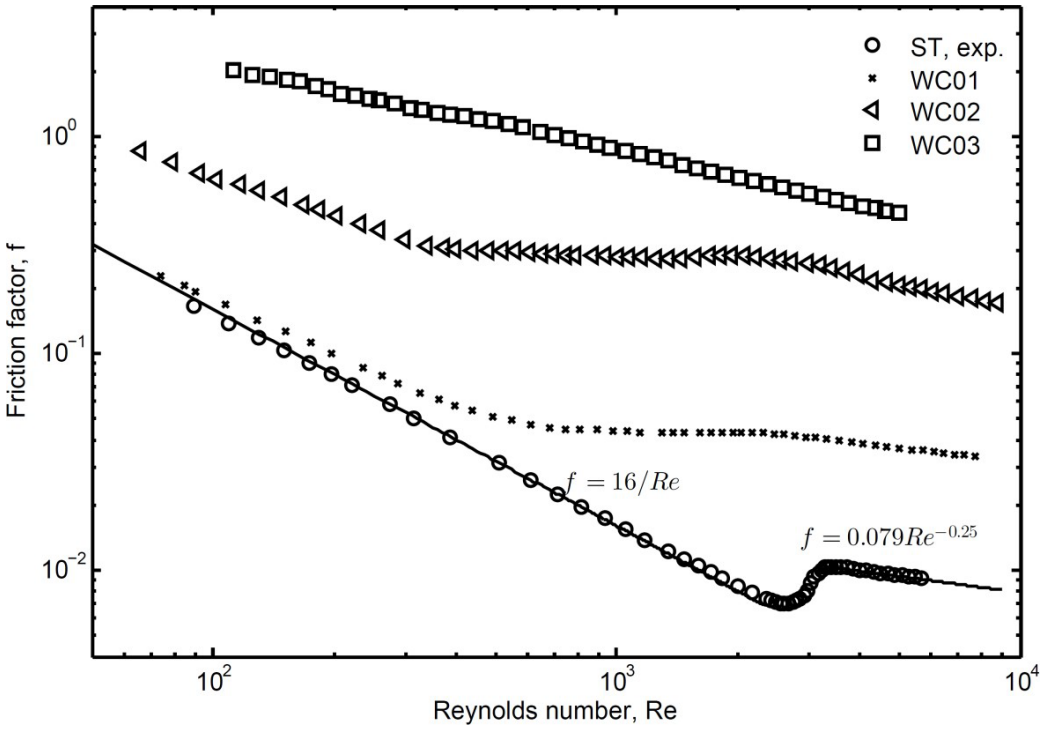

Figure 5: Comparison of wire coils and smooth tube isothermal friction factor

It is clearly observed that WC01 and WC02 produce an early transition to turbulent flow. This is shown in the friction factors curves that clearly indicate the presence of transitional turbulent flow regime as Re increases. This behaviour was reported by García et al [17] in a flow visualization work, where a low Re turbulent flow regime was observed with the presence of a peripheral region flow following wire pitch direction. This behaviour differs from the previously observed within twisted-tape inserts. Critical Reynolds numbers are reached at Re≈700 for WC01 and Re≈400 for WC02.

WC03 exhibits a different behaviour. As a change of trend is not seen, a transition to laminar flow cannot be inferred. The extreme wire-coil geometry (p/e=3.5) reduces the useful cross-section of the tube which increases the velocity in the central pipe region (increasing effective Re). This means that turbulent flow occurs at lower mass flow rates values than the other inserts. Therefore much higher values of friction factor are observed.

Table 4 presents the rise in insert friction factor in terms of f_i/f_s ratio. WC01 shows the smallest increase at the whole range of Re numbers analysed. This is followed by the twisted tapes inserts, in which the friction factors ratios increase for decreasing twist ratio. WC03 offers the highest values by far. WC02 has high friction factors in between WC03 and TT03.

However, the most significant behaviour is where the fluid flow matches the Reynolds numbers of operational solar collectors.. For Re=1000, WC01 works under turbulent regime at the minimum friction expense ratio of 2.8. The lowest twist ratio tape (TT01) presents a 1.7-fold higher friction factor than WC01. WC03 presents the extreme value reaching 55 times smooth tube friction factor. WC02 shows a 2-fold ratio increment regarding TT03.

Table 4. Friction factor ratio values f_i/f_s.

	TT01	TT02	TT03	WC01	WC02	WC03
Re	f_i/f_s	f_i/f_s	f_i/f_s	f_i/f_s	f_i/f_s	f_i/f_s
300	3.9	4.1	4.8	1.3	6.0	24.9
500	4.0	4.5	6.4	1.6	10.0	37.2
1000	4.8	5.8	8.2	2.8	18.2	55.0
1500	5.6	6.8	9.6	4.0	24.9	67.1
2000	6.0	7.8	12.0	5.0	35.1	79.8

In general, twisted-tapes give more moderate friction factor increments. This is due to the flow laminarization effect in contrast to the wire coil turbulence promotion effect. Despite being under laminar flow, the presence of a twisted tape within a tube causes an increase on friction factor due to tube blockage and partitioning, these facts decrease the hydraulic diameter and increase the flow velocity and effective flow path.

Although a small diameter wire coil (such as WC01) promotes transition to turbulence with a hydraulic diameter similar to that of a smooth pipe, under laminar flow it has very low friction factor values and even for turbulent regime it maintains low friction factor values, lower than the encountered for twisted tapes.

On the other hand, the wire coils with higher diameters have strongly increased friction factors. A limit case would be WC03. The aforementioned fact makes it unsuitable for use in serpentine-type solar collectors where the pressure loss introduced by an insert is a vital design factor.

In parallel-type solar collectors, although the inserts increase pressure drop inside the risers, this accounts for a small fraction of the overall pressure loss along solar collector itself. Furthermore, the solar collector itself just computes for less than a 20% of the total head in a practical installation. Thus, in harp-type collectors the increment in pressure drop originated by the inserts is not a determining factor, and the insert selection main consideration should be the resulting increase on thermal efficiency. ([14])

3.2 Heat transfer results

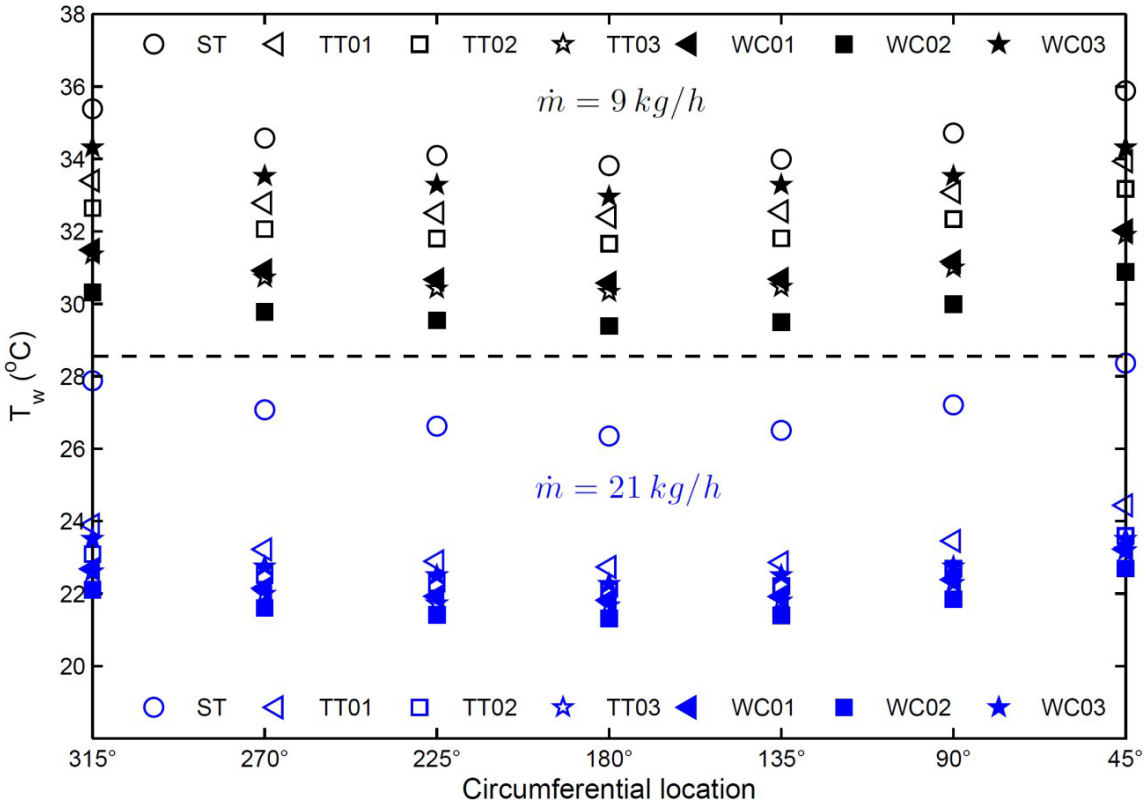

Figure 6. Peripheral tube wall temperature distribution at section J (fully-developed region)

Fig. 6 shows the peripheral tube wall temperature distribution for mass flow rates 9 and 21 kg/h, respectively at section J (axial position of 1610 mm) where fully hydraulic and thermal developed flow is encountered.

There is a lack of uniformity in tube wall temperature distribution. The lowest value is achieved at the circumferential location: 180° (bottom horizontal). Temperature rises at closer locations to the absorber panel inserts reduce circumferential temperature gradients although they do not suppress it completely.

For the lowest mass flow of 9 kg/h (Re≈485), all the inserts reduce wall temperature with regard to the smooth tube but, depending on the insert geometry they show a clearly distinguished behaviour. WC02, under turbulent flow according to friction factor results, exhibit the lowest tube wall temperatures. WC01 and TT03 show similar results. TT03 would be, according to Sw values, under swirl flow regime with a fully established tape-twist-induced swirl. And, WC01 would be under a laminar undulating flow with turbulence outbreaks (according to [17])). TT01 and TT02 have intermediate temperature values. Both devices present lower Sw numbers and would be under a viscous flow regime beginning the onset and growth of swirl. The worst thermal behaviour is exhibited by WC03. Unluckily, despite highly perturbing the flow, the existence of flow attached to the walls at lower mass flows induces an extra thermal resistance and poorer thermal characteristics.

For the most representative mass flow of 21 kg/h, a general decrease in wall temperature is encountered even for the smooth tube. It is remarkable that in contrast to the behaviour reported for the lowest mass flow rate, all the inserts group together and cause a pronounced decrease in wall temperature with respect to the smooth tube. The best insert device is WC02 then TT03 and WC01, followed by TT02 and WC03 with similar wall temperature values and finally TT01 (largest pitch twisted-tape).

The twisted tapes show an improved thermal behaviour for rising Swirl numbers, where fully developed swirl regime is achieved (Sw>250). The formation of helical swirl is the predominant convection mechanism and cross-stream mixing and sharper wall gradients are promoted. This mechanism is presented for TT03 and TT02 but not for TT01 which is under a different flow regime i.e a swirl-transition regime in which the onset and growth of swirl regime is taken place. The explanation for the good thermal characteristics shown by WC01 and WC02 lies in the development of turbulent flow regime. Regarding WC03, for this Re number the central turbulent flow is able to mix in the secondary peripheral flow adhered to the wall. Wall thermal resistance is progressively reduced as the mass flow rate rises. This explains the different thermal behaviour observed when comparing the two mass flowrates under analysis.

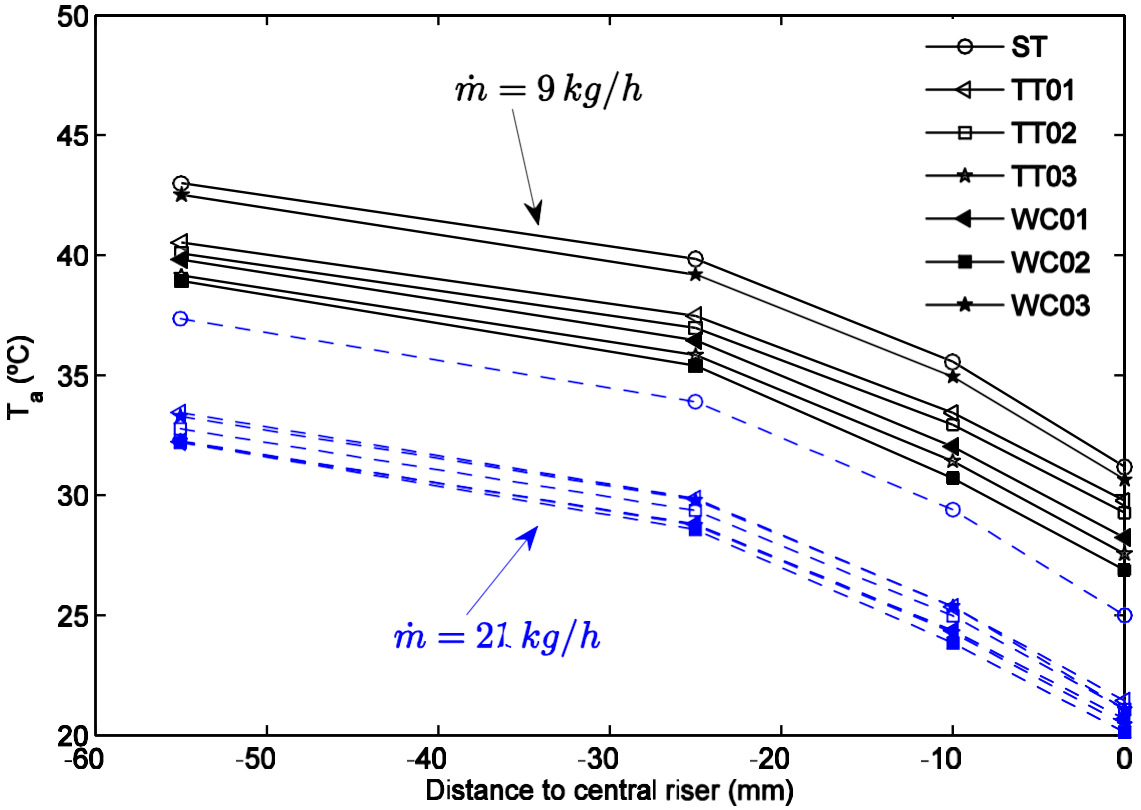

Figure 7. Temperature profile in the absorber cross section and at the bottom of the central riser (x=1290 mm).

Fig. 7 depicts the temperature profile in the absorber cross section located at the left of the central riser (at -55 mm, -25 mm and -10 mm) and at the lowest tube circumferential location of the riser (x=0, 180°).

The increase in the convective heat transfer coefficients in the riser due to the inserts causes a decrease in the temperature distribution of the absorber panel. As previously reported, for the lowest mass flows the different inserts show a well differentiated behaviour while at higher mass flow the inserts group together and are able to substantially reduce temperature. When temperature is reduced along the whole absorber panel a significant impact on the thermal efficiency of the solar collector would be expected, taking into account the dependency of this parameter with the thermal loses to the ambient.

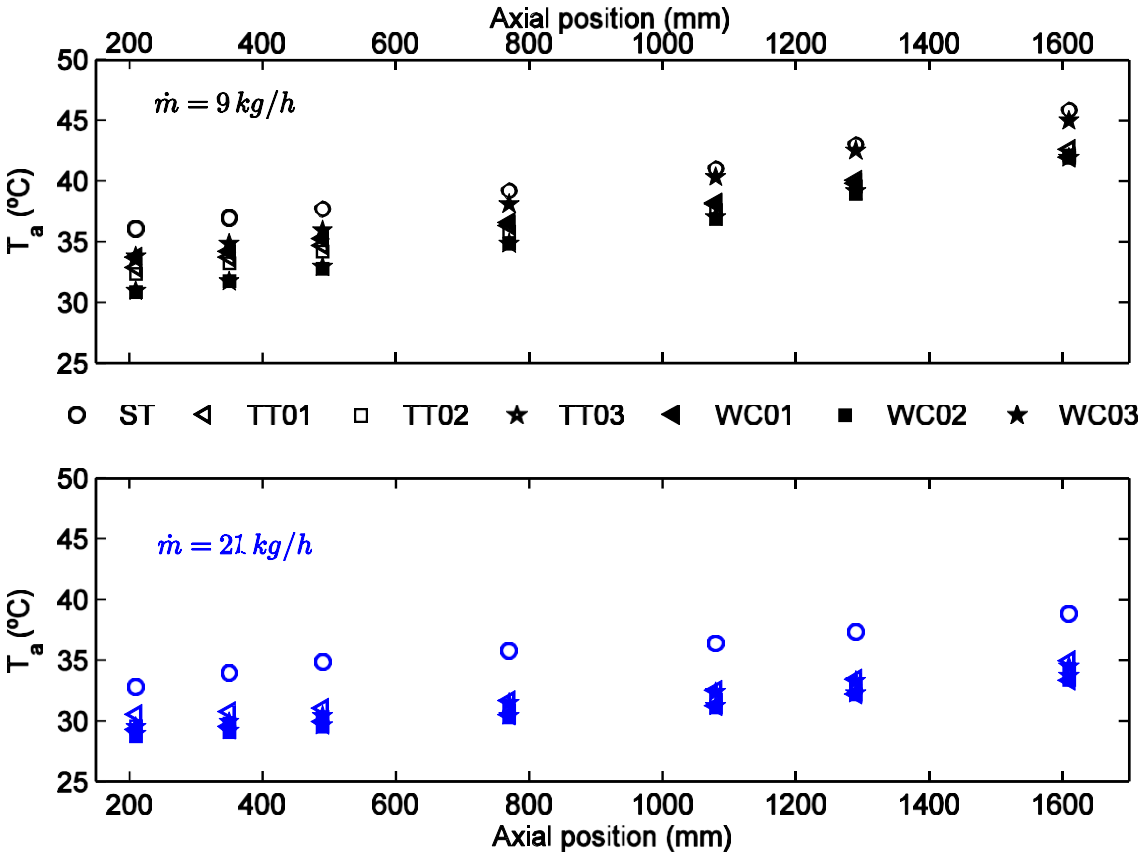

Figure 8. Axial evolution of temperature profile along the absorber plate.

In Fig. 8 the axial evolution of temperature profiles along the absorber in its middle point (section A) between adjacent risers is represented. It is clearly observed how the inserts decrease temperature from the absorber entrance. It can be easily seen that there is a significant impact in temperature over the whole absorber. Nevertheless, this behaviour is clearly different and dependent on the operating conditions (mass flow rate and type of insert specimen). For the lowest mass flow rate, WC03 shows a moderate decrease on absorber temperature. However, in the typical solar collector operating conditions (21 kg/h) all the specimens show a positive thermal behaviour (See Table 5).

Table 5. Average temperature drop ($T_{a,i}$-$T_{a,s}$) along the absorber plate, for enhanced and smooth tubes.

	$\dot{m}_1 = 9$ kg/h	$\dot{m}_1 = 13$ kg/h	$\dot{m}_1 = 21$ kg/h	$\dot{m}_1 = 32$ kg/h	$\dot{m}_1 = 50$ kg/h
TT01(˚C)	3.06	2.68	3.57	4.16	3.37
TT02(˚C)	3.56	3.56	4.37	4.52	3.74
TT03(˚C)	4.47	4.80	4.95	5.05	4.22
WC01(˚C)	2.87	4.18	4.84	5.40	4.79
WC02(˚C)	4.55	4.98	5.09	5.34	4.06
WC03(˚C)	1.33	2.98	4.07	4.97	4.15

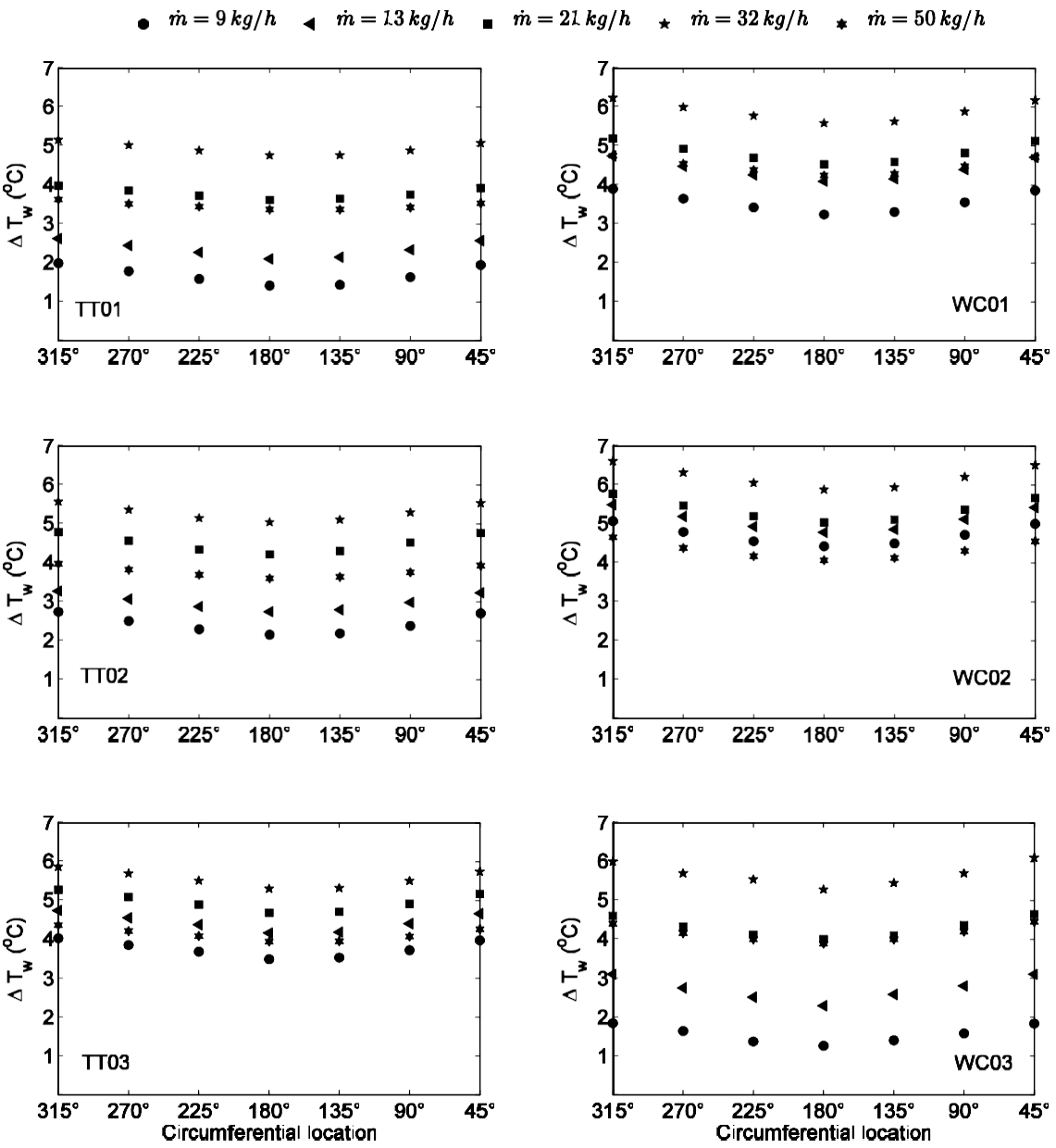

Figure 9. Wall temperature differences (insert vs smooth tube) at section J for all the mass flows studied.

In order to enable a global vision of the work carried out and to easily compare each insert behaviour under all the operating conditions (five different mass flow rates), Fig. 9 shows the wall temperature reduction of each device in comparison with smooth tube at section J.

Overall, the worst thermal performance is observed for TT02, WC03 and TT01 which show a strong dependence on mass flow rate and lower values of ΔT_w (See Table 6). The best specimens are WC01, WC02 and TT03, due to their capacity to disturb the flow at low Reynolds numbers, whereas, the worst are not able to disturb the flow until medium range Re numbers. From a certain Re (Re≈1000, 21 kg/h), the flow is adequately disturbed which gives a good performance for all inserts, the maximum output is achieved at Re≈1500 (32 kg/h) and then a decrease is observed (Re≈2300), this corresponds to to the point that a turbulent flow regime is achieved in the smooth pipe.

Table 6. Average temperature drop ($\Delta T_w=T_{W,i}-T_{w,s}$) at section J for different mass flows

	$\dot{m}_1 = 9$ kg/h	$\dot{m}_1 = 13$ kg/h	$\dot{m}_1 = 21$ kg/h	$\dot{m}_1 = 32$ kg/h	$\dot{m}_1 = 50$ kg/h
Re	400-570	570-740	930-1050	1400-1600	2200-2500
TT01(˚C)	1.68	2.36	3.79	4.94	3.47
TT02(˚C)	2.42	3.00	4.50	5.29	3.77
TT03(˚C)	3.75	4.44	4.96	5.56	4.13
WC01(˚C)	3.56	4.41	4.84	5.90	4.49
WC02(˚C)	4.73	5.11	5.37	6.22	4.32
WC03(˚C)	1.64	3.30	4.82	6.31	4.83

4. Conclusions

- All the studied insert devices increase pressure drop inside the riser and decrease absorber plate temperature for all the operating conditions. However, noticeably different behaviours are reported according to insert geometry and flow conditions.
- Regarding pressure drop, twisted tapes present moderate increments whereas wire-coils strongly depend on their geometrical characteristics. For a typical laminar flow regime in solar collectors of Re=1000, the friction ratios (f_i/f_s) computed are 4.8 for TT01, 5.8 for TT02 and 8.2 for TT03 and 2.8, 18.2 and 55.0 for WC01, WC02 and WC03, respectively. The less severe wire-coil insert offers the lowest pressure drop results among all the inserts studied.
- The increase in the tube-side heat transfer convective coefficient is reflected on the reduction of the average peripheral wall temperature reduction (insert vs smooth tube). From Re≈1000 (21 kg/h) all inserts show good performance. The maximum average ΔT_w computed for Re≈1500 are 4.94˚C for TT01, 5.29˚C for TT02, 5.56˚C for TT03, 5.90˚C for WC01, 6.22˚C for WC02 and 6.31˚C for WC03. When the smooth tube reaches turbulent flow regime (Re≈2300) a decrease on wall temperature differences is observed.
- This increase on the inner heat transfer coefficient causes an important decrease on the absorber temperature. The best inserts (wire coils WC02, WC01 and twisted tape TT03) have an excellent behaviour for any flow condition, whereas other inserts present moderate reductions for the lower mass flow rates. With increasing mass flow rates all the inserts present a very similar performance. In the typical solar collector operating conditions (21 kg/h) the average values of temperature profile along the absorber plate are 3.57˚C for TT01, 4.37˚C for TT02, 4.95˚C for TT03, 4.84˚C for WC01, 5.09˚C for WC02 and 4.07˚C for WC03. It is expected that this fact have a positive effect in terms of an increase in a real solar collector thermal efficiency.
- All the inserts studied can be successfully implemented on harp-type solar collectors for the typical solar collector operating conditions with no constraints. Nevertheless, the best inserts are WC01, WC02 and TT03 since they show important decreases on the absorber temperatures through all the operating mass flow rates. Regarding serpentine type collectors, only the best inserts in terms of pressure drop increase (a priority concern) and thermal behaviour can be used to enhance heat transfer. Regarding the present study, the WC01 (p/d=1.5 and e/d=0.07) would be the best specimen to insert according to its moderate pressure drop rise (f_i/f_s =2.8 at Re≈1000)

and its early promotion of turbulent flow at Re≈700, that greatly reduces the absorber wall temperature (4.84°C at Re≈1000).

Acknowledgements

The authors gratefully acknowledge the “Agencia de Ciencia y Tecnología de la Región de Murcia” (Fundación Séneca: Project with Ref. 15297/PI/10) and the Spanish Ministry of Science (Project with Ref. ENE2011-28571-C02-01) for supporting this research.

5. References

[1] J.A. Duffie, W.A. Beckman, Solar Engineering of Thermal Processes, third ed., John Wiley and Sons, Hoboken, New Jersey, USA, 2006.

[2] Pandey K M, Chaurasiya R, A review on analysis and development of solar flat plate collector, In Renewable and Sustainable Energy Reviews, Volume 67, 2017, Pages 641-650, ISSN 1364-0321, https://doi.org/10.1016/j.rser.2016.09.078.

[3] Shuilian Li, Hui Wang, Xiangrui Meng, Xinli Wei, Comparative study on the performance of a new solar air collector with different surface shapes, In Applied Thermal Engineering, Volume 114, 2017, Pages 639-644, ISSN 1359-4311, https://doi.org/10.1016/j.applthermaleng.2016.12.026.

[4] Sompol Skullong, Pongjet Promvonge, Chinaruk Thianpong, Nuthvipa Jayranaiwachira, Monsak Pimsarn, Heat transfer augmentation in a solar air heater channel with combined winglets and wavy grooves on absorber plate, In Applied Thermal Engineering, Volume 122, 2017, Pages 268-284, ISSN 1359-4311, https://doi.org/10.1016/j.applthermaleng.2017.04.158.

[5] Ravi Kant Ravi, R.P. Saini, Nusselt number and friction factor correlations for forced convective type counter flow solar air heater having discrete multi V shaped and staggered rib roughness on both sides of the absorber plate, In Applied Thermal Engineering, Volume 129, 2018, Pages 735-746, ISSN 1359-4311, https://doi.org/10.1016/j.applthermaleng.2017.10.080.

[6] Tingting Zhu, Yanhua Diao, Yaohua Zhao, Cheng Ma, Performance evaluation of a novel flat-plate solar air collector with micro-heat pipe arrays (MHPA), In Applied Thermal Engineering, Volume 118, 2017, Pages 1-16, ISSN 1359-4311, https://doi.org/10.1016/j.applthermaleng.2017.02.076.

[7] H. Javaniyan Jouybari, S. Saedodin, A. Zamzamian, M. Eshagh Nimvari, Experimental investigation of thermal performance and entropy generation of a flat-plate solar collector filled with porous media, In Applied Thermal Engineering, 2017, Volume 127, Pages 1506-1517, ISSN 1359-4311, https://doi.org/10.1016/j.applthermaleng.2017.08.170.

[8] Hajabdollahi F., Premnath K., Numerical study of the effect of nanoparticles on thermoeconomic improvement of a solar flat plate collector, Applied Thermal Engineering, 2017,127: 390-401, https://doi.org/10.1016/j.applthermaleng.2017.08.058.

[9] Farzaneh Hajabdollahi, Kannan Premnath, Numerical study of the effect of nanoparticles on thermoeconomic improvement of a solar flat plate collector, Applied Thermal Engineering, Volume 127, 25 December 2017, Pages 390-401, ISSN 1359-4311, https://doi.org/10.1016/j.applthermaleng.2017.08.058.

[10] Sujit Kumar Verma, Arun Kumar Tiwari, Durg Singh Chauhan, Experimental evaluation of flat plate solar collector using nanofluids, Energy Conversion and Management, Volume 134, 15 February 2017, Pages 103-115, ISSN 0196-8904, https://doi.org/10.1016/j.enconman.2016.12.037.

[11] M.A. Sharafeldin, Gyula Gróf, Experimental investigation of flat plate solar collector using CeO_2-water nanofluid, Energy Conversion and Management, Volume 155, 1 January 2018, Pages 32-41, ISSN 0196-8904, https://doi.org/10.1016/j.enconman.2017.10.070.

[12] Javaniyan Jouybaria H., Saedodina S, Zamzamianb, A., Eshagh Nimvaric M., Wongwisesd S., Effects of porous material and nanoparticles on the thermal performance of a flat plate solar collector: An experimental study Renewable Energy 2017 Volume 114, Part B,: 1407–1418 https://doi.org/10.1016/j.renene.2017.07.008

[13] S. Sadhishkumar, T. Balusamy, Performance improvement in solar water heating systems—A review, Renewable and Sustainable Energy Reviews, 37 (2014), 191-198. http://dx.doi.org/10.1016/j.rser.2014.04.072

[14] K. Balaji, S. Iniyan, Ranko Goic, Thermal performance of solar water heater using velocity enhancer, In Renewable Energy, Volume 115, 2018, Pages 887-895, https://doi.org/10.1016/j.renene.2017.09.014.

[15] K. Balaji, S. Iniyan, V. Muthusamyswami, Experimental investigation on heat transfer and pumping power of forced circulation flat plate solar collector using heat transfer enhancer in absorber tube, In Applied Thermal Engineering, Volume 112, 2017, Pages 237-247, https://doi.org/10.1016/j.applthermaleng.2016.09.074.

[16] S. Suman, M. K. Khan, M. Pathak, Performance enhancement of solar collectors—A review, Renewable and Sustainable Energy Reviews, 49 (2015) 192-210. http://dx.doi.org/10.1016/j.rser.2015.04.087

[17] Bergles AE, Manglik RM. Enhanced Heat Transfer in Single-Phase Forced Convection in Tubes due to Helical Swirl Generated by Twisted-Tape Inserts. ASME. Heat Transfer Summer Conference, Volume 2: Heat Transfer Enhancement for Practical Applications; Fire and Combustion; Multi-Phase Systems; Heat Transfer in Electronic Equipment; Low Temperature Heat Transfer; Computational Heat Transfer (2012):77-86. doi:10.1115/HT2012-58285.

[18] Manglik RM., Maramraju S., Bergles AE, The Scaling and Correlation of Low Reynolds Number Swirl Flows and Friction Factors in Circular Tubes with Twisted-Tape Inserts.
Journal of Enhanced Heat Transfer (2001) Vol 8: 383-395. DOI: 10.1615/JEnhHeatTransf.v8.i6.30

[19] A. Kumar, B.N. Prasad, Investigation of twisted tape inserted solar water heaters: heat transfer, friction factor and thermal performance results, Renewable Energy 19 (2000) 379-398. http://dx.doi.org/10.1016/S0960-1481(99)00061-0

[20] S. Jaisankar, T.K. Radhakrishnan, K.N. Sheeba, Experimental studies on heat transfer and friction factor characteristics of forced circulation solar water heater

system fitted with helical twisted tapes, Solar Energy 83 (2009) 1943-1952. http://dx.doi.org/10.1016/j.solener.2009.07.006

[21] V. Pavendan, K. Muthukumar, N.Arivazhagan, K. Srithar, Heat transfer augmentation in a solar water heater using cross and twisted tape inserts. International Journal of Applied Engineering Research 2015, Volume 10, Issue 6, Pages 14739-14754

[22] L. S. Sundar, Manoj K. Singh, V. Punnaiah, Antonio C.M. Sousa, Experimental investigation of Al_2O_3/water nanofluids on the effectiveness of solar flat-plate collectors with and without twisted tape inserts, In Renewable Energy, 2017, https://doi.org/10.1016/j.renene.2017.10.056.

[23] S. Jaisankar, TK Radhakrishnan, KN Sheeba. Experimental studies on heat transfer and thermal performance characteristics of thermosyphon solar and thermal performance characteristics of thermosiphon solar water heating system with helical and left -right twisted tapes. Energy Convers Manag 52 Issue 5 (2011) 2048-2055. http://dx.doi.org/10.1016/j.enconman.2010.11.024

[24] S Jaisankar, TK Radhakrishnan, KN Sheeba, S Suresh. Experimental investigation of heat transfer and friction factor characteristics of thermosiphon solar water heater system fitted with spacer at the trailing edge of left-right twisted tapes. Energy Convers Manag 50 Issue 10 (2009) 2638-2649. http://dx.doi.org/10.1016/j.enconman.2009.06.019

[25] S Jaisankar, TK Radhakrishnan, KN Sheeba. Experimental studies on heat transfer and friction factor characteristics of thermosiphon solar water heater system fitted with spacer at the trailing edge of twisted tapes. Appl Therm Eng 29 Issue 5-6 (2009) 1224-1231. http://dx.doi.org/10.1016/j.applthermaleng.2008.06.009

[26] S Jaisankar, TK Radhakrishnan, KN Sheeba. Studies on heat transfer and friction factor characteristics of thermosiphon solar water heating system with helical twisted tapes. Energy, 34 Issue 9 (2009) 1054-1064. http://dx.doi.org/10.1016/j.energy.2009.03.015

[27] J. Ananth, S Jaisankar. Investigation on heat transfer and friction factor characteristics of thermosiphon solar water heating system with left-right twist regularly spaced with rod and spacer. Energy, 65 Issue 1 (2014) 357-363. http://dx.doi.org/10.1016/j.energy.2013.12.001

[28] S. Jaisankar, T.K. Radhakrishnan, K.N. Sheeba, Studies on heat transfer and friction factor characteristics of thermosyphon solar water heating system with helical twisted tapes, Energy 34 (2009) 1054-1064. http://dx.doi.org/10.1016/j.energy.2009.03.015

[29] A. Saravanan, J.S. Senthilkumaar, S. Jaisankar, Performance assessment in V-trough solar water heater fitted with square and V-cut twisted tape inserts, In Applied Thermal Engineering, Volume 102, 2016, Pages 476-486, ISSN 1359-4311, https://doi.org/10.1016/j.applthermaleng.2016.03.088.

[30] A. Saravanan, J.S. Senthilkumaar, S. Jaisankar, Experimental studies on heat transfer and friction factor characteristics of twist inserted V-trough thermosyphon solar water heating system, In Energy, Volume 112, 2016, Pages 642-654, ISSN 0360-5442, https://doi.org/10.1016/j.energy.2016.06.103.

[31] M Sheikholeslami, M Gorji-Bandpy, D. D. Ganji, Review of heat transfer enhancement methods: Focus on passive methods using swirl flow devices. Renewable and Sustainable Energy Reviews, 49 (2015) 444–469. http://dx.doi.org/10.1016/j.rser.2015.04.113

[32] A. García, J.P. Solano, P.G. Vicente, A. Viedma, The influence of artificial roughness shape on heat transfer enhancement: Corrugated tubes, dimpled tubes and wire coils, In Applied Thermal Engineering, Volume 35, 2012, Pages 196-201, ISSN 1359-4311, https://doi.org/10.1016/j.applthermaleng.2011.10.030.

[33] A. García, J.P. Solano, P.G. Vicente, A. Viedma, The influence of artificial roughness shape on heat transfer enhancement: Corrugated tubes, dimpled tubes and wire coils, In Applied Thermal Engineering, Volume 35, 2012, Pages 196-201, https://doi.org/10.1016/j.applthermaleng.2011.10.030.

[34] T.S. Ravigururajan, T.J. Rabas, Turbulent flow in integrally enhanced tubes, Part 2: analysis and performance comparison, Heat Transfer Eng. 17 (1996) 30–40, http://dx.doi.org/10.1080/01457639608939871.

[35] A. García, J.P. Solano, P.G. Vicente, A. Viedma, Flow pattern assessment in tubes with wire coil inserts in laminar and transition regimes, In International Journal of Heat and Fluid Flow, Volume 28, Issue 3, 2007, Pages 516-525, https://doi.org/10.1016/j.ijheatfluidflow.2006.07.001.

[36] J. Pérez-García, A. García, R. Herrero-Martín, J.P. Solano, Experimental correlations on critical Reynolds numbers and friction factor in tubes with wire-coil inserts in laminar, transitional and low turbulent flow regimes, In Experimental Thermal and Fluid Science, Volume 91, 2018, Pages 64-79, , https://doi.org/10.1016/j.expthermflusci.2017.10.003.

[37] R. Herrero Martín, J. Pérez-García, A. García, F.J. García-Soto, E. López-Galiana. Simulation of an enhanced flat-plate solar liquid collector with wire-coil insert devices. Solar Energy 85 Issue 3(2011) 455-469. http://dx.doi.org/10.1016/j.solener.2010.12.013

[38] A. García, R Herrero Martin, J. Pérez-García. Experimental study of heat transfer enhancement in a flat-plate solar water collector with wire-coil inserts. Applied Thermal Engineering, 61, Issue 2-3 (2013) 461-468. http://dx.doi.org/10.1016/j.applthermaleng.2013.07.048

[39] A. Huertas, J. P. Solano, A. Garcia, R. Herrero-Martín, and J. Pérez-García, “Tube-side heat transfer enhancement in flat-plate liquid solar collectors with wire coil inserts” Experimental Heat Transfer Vol. 30 Iss. 1,(2015) http://dx.doi.org/10.1080/08916152.2015.1124156

[40] A Hobbi, K. Siddiqui,. Experimental study on the effect of heat transfer enhancement devices in flat-plate solar collectors. International Journal of Heat and Mass Transfer 52 Issue 19–20, (2009) 4650–4658. http://dx.doi.org/10.1016/j.ijheatmasstransfer.2009.03.018

[41] G. Sandhu, K. Siddiqui, A. Garcia, Experimental study on the combined effects of inclination angle and insert devices on the performance of a flat-plate solar collector. International Journal of Heat and Mass Transfer, 71 (2014) 251-263. http://dx.doi.org/10.1016/j.ijheatmasstransfer.2013.12.004

[42] Manglik R. M. and Bergles A. E. Heat Transfer and Pressure Drop Correlations for Twisted-Tape Inserts in Isothermal Tubes: Part II—Transition and Turbulent Flows J. Heat Transfer 115(4) (1993) 890-896 doi:10.1115/1.2911384
Manglik R. M. and Bergles A. E. Characterization of Twisted-Tape-Induced Helical Swirl Flows for Enhancement of Forced Convective Heat Transfer in Single-Phase and Two-Phase Flows. J. Thermal Sci. Eng. Appl 5(2), (2013) 021010-12 pages Paper No: TSEA-12-1204; doi: 10.1115/1.4023935